sustainability

Article

Safety Analysis and Emergency Response of Suspended Oil and Gas Pipelines Triggered by Natural Disasters

Jin Yu [1], Chao Chen [2,*] and Changjun Li [2]

[1] China National Offshore Oil Corporation, Beijing 100010, China
[2] School of Petroleum Engineering, Southwest Petroleum University, Chengdu 610500, China
* Correspondence: chenchaoswpu@gmail.com

Abstract: Pipelines play a dominant role in the transportation of oil and gas and the safety of pipelines is essential for the supply of energy. However, natural disasters such as floods and land subsidence may lead to suspended pipelines, resulting in pipeline failure accidents, causing casualties and environmental pollution. To deal with the emergency caused by suspended pipelines, it is needed to identify the failure mechanisms of suspended pipelines caused by natural disasters. Therefore, this study conducts a safety analysis of suspended pipelines using a nonlinear finite element method (FEM), considering the nonlinear pipe–soil contact and plastic deformation. A case study is conducted to investigate the influencing parameters (e.g., the suspended length, the operating pressure, and the fluid mass). This work demonstrates that irreversible plastic strains occur when the suspended length exceeds 50 m, and it will reach 2% when the suspended length is 340 m. Finally, an emergency response plan based on plastic strain and suspended length is proposed to determine the emergency level of the suspended pipelines caused by natural disasters. This study can provide technical support for the emergency response of pipelines in areas with frequent natural disasters, promoting the sustainable development of oil and natural gas pipelines.

Keywords: pipeline; safety; suspended length; natural disasters; emergency response; plastic strain

Citation: Yu, J.; Chen, C.; Li, C. Safety Analysis and Emergency Response of Suspended Oil and Gas Pipelines Triggered by Natural Disasters. *Sustainability* **2022**, *14*, 17045. https://doi.org/10.3390/su142417045

Academic Editor: Md Mizanur Rahman

Received: 15 November 2022
Accepted: 15 December 2022
Published: 19 December 2022

1. Introduction

Oil and gas play a dominant role in modern industry and fife, accounting for 53% of the used primary energies in the whole world in 2021 [1,2]. Pipelines play a dominant role in the transportation of oil and gas, playing an essential role in energy supply. However, oil and gas pipelines always cross different landforms such as mountains, rivers, marshes, plateaus, cities, and permafrost, exposed to different accidental hazards and natural hazards [3–6]. Natural disasters such as floods and land subsidence and earthquakes may cause local ground collapse or subsidence, resulting in a suspended pipeline. For instance, in 2013, a flood caused by a rainstorm damaged the soil around a refined oil pipeline in Sichuan, China, resulting in a suspended pipeline and the interruption of the oil supply [7]. In 2014, a natural gas pipeline suddenly leaked due to ground subsidence, and many people were evacuated to avoid casualties [8]. Without the support of foundations, the mechanical properties and deformation distribution of the suspended pipe resulting from natural disasters may dramatically change, resulting in the fracture of pipelines. The fracture of pipelines leads to leakage of hydrocarbon products and the interruption of energy supply, and possibly causes explosions or fire, resulting in more severe consequences. For example, the accident of a suspended pipeline. Excessive plastic deformation occurred without the support of soil, threatening the safety operation of the refined oil. However, without reliable safety assessment methods, the emergency response plans were not rapidly developed, resulting in a long interruption of refined oil transportation and economic losses.

In light of the severe consequences of suspended pipelines caused by natural disasters, failure analysis using advanced techniques is vital to determine the safety level of suspended pipelines and formulate an emergency response plan. However, past research mainly focuses on the span analysis of offshore pipelines [9], and the failure analysis of suspended pipelines is invariably ignored. Wu et al. [10] analyzed suspended pipes by using CAESAR II software, while the software is a pipeline design software that cannot obtain the precise and fine stress and strain distribution of pipelines and fully reflect the failure mechanisms. In the pipeline stress analysis domain, simplified analytical methods are always used for design while advanced finite element methods are the main methods to investigate the failure mechanism caused by nature disasters [11]. Peng and Luo [12] proposed a beam-bending model for calculating the stress status of the suspended pipe resulting from soil subsidence. Cao et al. [13] obtained a similar model for underground pipelines due to the operation of mines. Karamitros et al. [14] proposed a stress calculation technique for pipes that cross multiple faults. Hendriks et al. [15] calculated the strain state of a pipe subjected to land sinks by developing mathematical models. Mathematical models for analyzing pipes exposed to faults were also developed [16,17]. Additionally, Zhang et al. [18] investigated the stress of a pipe exposed to landslides triggered by rains by establishing an analytical model based on the Pasternak two-parameter model. Liao et al. [19] employed a beam bending model and finite element method to analyze the long-span suspended pipeline stress deformation.

In addition to analytical methods, more attention has been paid to finite element methods (FEM) to model the nonlinear mechanical behaviors of plastic deformation and pipe–soil contact [20–22]. The nonlinear FEM has been extensively used for failure analysis of buried pipelines under geological disasters. Wang et al. [23] analyzed the suspended pipeline deformation, stress, and strain by a finite element method. Zakeri [24] employed CFD for analyzing a subsea pipe considering the drag forces caused by the ocean current. Shao et al. [25] presented a nonlinear FE model for analyzing a subsea pipe, considering the effects of submarine mud. Kunert et al. [26] proposed a nonlinear FEM strategy for calculating the stress of pipes located in rainy-forest areas. Zhang et al. [27] investigated the rupture of welded pipes with cracks by using a nonlinear numerical method. Saeedzadeh and Hataf [28] presented a numerical study of the assessment of the influence of soil properties and field conditions in pipeline floatation. Zheng et al. [29] analyzed the stress of pipelines caused by landslides by using a nonlinear algorithm in FEM. Zhang et al. [30] investigated the bulking behavior of buried gas pipelines under strike–slip fault displacement by a finite element method. Liu et al. [31] analyzed the stress and failure of pipelines in the lifting process by a finite element method. Vazouras et al. [32] combined a FEM and an analytical method to investigate the stress status of pipes exposed to faults. Tavakoli Mehrjardi and Karimi [33] conducted a finite element method to analyze a buried steel pipe exposed to impact loads caused by rockfall and provided a suggested selection method for the buried depth of pipes to keep the safety of the pipe. Ma et al. [34] conducted a FEM to study the strain characteristics of a pipe exposed to landslides, and the results were almost identical to the results of strain test experiments. Cheng et al. [35] developed a FEM to explore the stress status of buried pipes in seafloors, considering the influence of buried depths. Tsatsis et al. [36] investigated pipe fragility exposed to slope failure-induced displacements using a finite element method and considering the uncertainty using fragility curves.

According to the above analysis, the safety status of suspended pipelines triggered by natural disasters is always ignored, and there is a lack of emergency response research for dealing with the suspended pipelines caused by natural disasters. In this study, a nonlinear finite element analysis for suspended pipelines due to natural disasters is performed, considering the nonlinear pipe–soil interaction and plastic deformation. The critical factors that may affect the safety status of suspended pipes are investigated based on FEM analysis. Additionally, a comparison between the results of the FEM analysis and the conservative analytic method is conducted, and a rupture risk index is developed to determine the emergency response levels. Finally, different emergency measures for different emergency levels are formulated for dealing with suspended pipelines triggered by natural disasters.

This paper consists of five sections. Section 2 introduces the materials and methods used for finite element analysis. Section 3 presents the results obtained from the FEM analysis and the analysis of critical factors. According to the simulation results, Section 4 establishes an emergency response plan for suspended pipelines caused by natural disasters. Finally, the conclusions drawn from the FEM analysis and emergency response research are summarized in Section 5.

2. Materials and Methods

The suspended pipeline triggered by natural disasters can be simplified as a pipeline with two rectangular soil masses at the ends of the pipeline, as shown in Figure 1. The geometric size of a soil mass is characterized by its length, width, and height. The pipe consists of three parts: the suspended section, the buried section on the left, and the buried section on the right. The buried depth indicates the length between the pipe centerline and the upper surface of the soil mass.

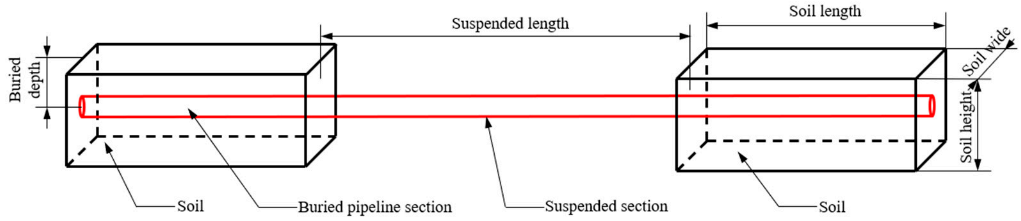

Figure 1. Geometric model of suspended pipeline triggered by natural disasters.

For investigating the rupture mechanism of suspended pipes, the parameters of a real suspended pipeline triggered by a flood are used as the input of the geometric model. The total pipe length is 480 m; the diameter equals 219.1 mm, with a wall thickness of 6.4 mm, including a suspended part is 320 m. The length of one side soil model is 80 m in length, 4 m in height, and 4 m in width, and the buried depth is 2 m. The transmission medium of the pipeline is oil; with a density of 840 kg/m^3. The internal pressure is 4 MPa. The pipe is produced by API X52 pipeline steel. This pipeline steel is always applied in low-medium pressure transport of oil and gas. Figure 2 shows the nonlinear relationship between the stress and strain of the pipeline steel. The yield strength σ_y is 375 MPa, and the other mechanical parameters are shown in Table 1.

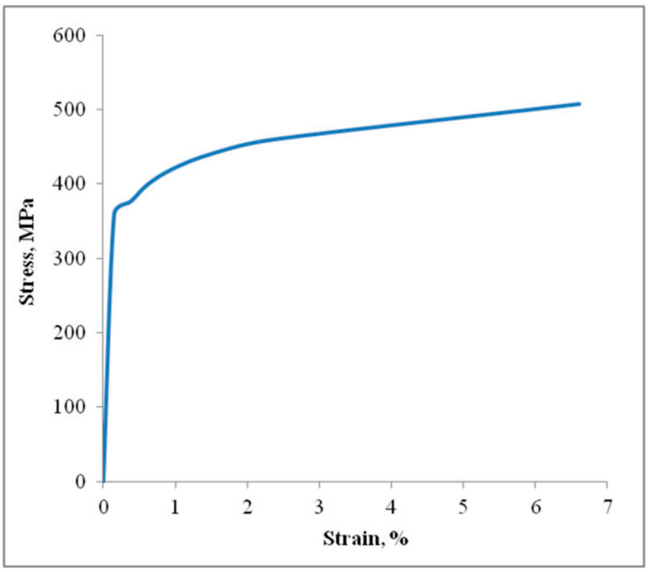

Figure 2. Stress-strain curve of X52 steel.

Table 1. Main parameters of the finite element model.

Parameters (Units)	Values
Soil length (m)	80
Soil depth (m)	2
Suspended length (m)	320
Pipeline diameter (mm)	219.1
Internal pressure (MPa)	4
Oil density (kg/m^3)	840
Pipeline material	X52 steel (API)
Yield strength (MPa)	375
Poisson's ratio	0.3
Elastic modulus (E)	203

The Drucker–Prager model is adopted for modeling soil behavior, since it is suitable to model soil's mechanical behaviors and is widely used to model the contact between the soil and pipelines [37,38]. According to the model, soil behavior is characterized by five parameters, and the values of the soil parameters are listed in Table 2.

Table 2. Soil model parameters.

P_s (kg/m^3)	E_s (Mpa)	v_s	c (kPa)	φ (°)	ψ (°)
1450	40	0.4	30	12.3	0

The analysis of the suspended pipelines is examined numerically by using the advanced computational software ANSYS [39]. An elasticplastic model with large-strain and isotropic is employed for the X52 pipeline. A frictional contact element is adopted to model the interface between the soil and the pipe. The element is described by friction coefficient, which is 0.3 in this study. The 3D finite element model is developed to investigate the stress status of the pipe, as shown in Figure 3. Eight-node and hexagonal grids are employed to mesh the pipeline and soil model, which includes 588,100 nodes and 273,822 nodes, respectively. Loads of the pipeline include its pipeline gravity, fluid gravity, and internal pressure besides the soil load. Three-step loads are added to the model in the solving process. The load sequence is as follows: pipeline gravity, fluid gravity, and internal pressure. The Augmented Lagrange method is selected as the nonlinear contact algorithm.

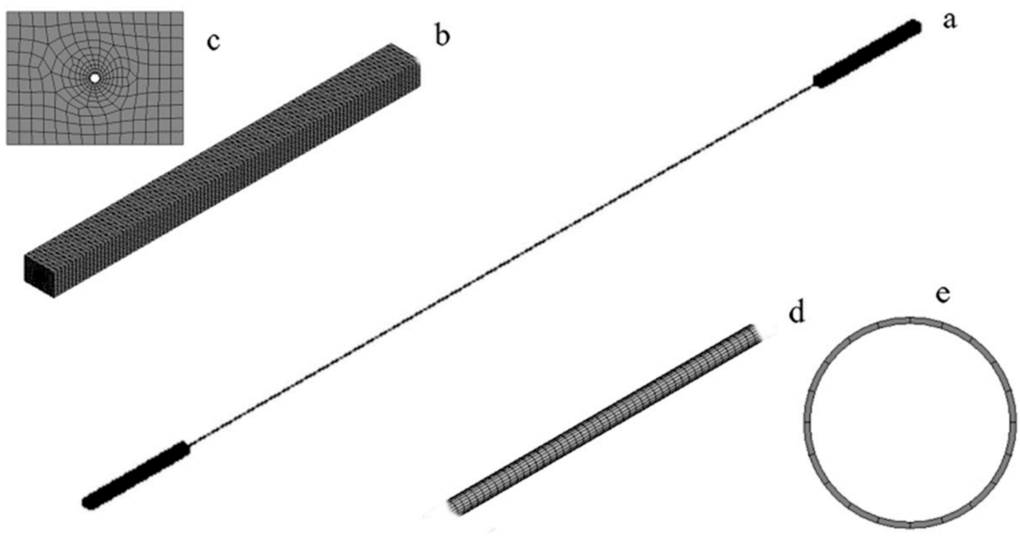

Figure 3. FEM model of the suspended pipeline triggered by floods.

The boundary conditions of this model are set according to the real pipeline conditions. The axial displacement of the pipe is fixed. The displacement of gravity direction of the soil bottom is fixed due to the support of lower soil.

3. FEM Analysis Results

The FEM model of the suspended pipeline with a length of 320 m is solved, considering the plastic nonlinear behavior of the pipeline steel and nonlinear contact between the pipeline and soil, as well as the pipe mass and the transferred oil. Figure 4 shows the equivalent stress along the pipeline. The stress concentration locations appear on both ends of the suspended pipeline section. The distribution of the equivalent, axial normal, and maximum principal stresses along the pipeline is shown in Figure 5a. The results indicate that the three stresses along the pipeline show similar varying tendencies, and the curve of the normal stress coincides with the curve of the principal stress. Therefore, the axial stress caused by the suspended pipeline is a leading factor in the process of pipeline failure. For the following analysis, both the equivalent stress and the axial normal stress are considered. The critical locations in which the ES exceeds the pipeline yield stress appear at both ends of the suspended section. The length of the critical location is 0.9 m, and the MES is 447.3 MPa, which is 1.19 times the yield limit.

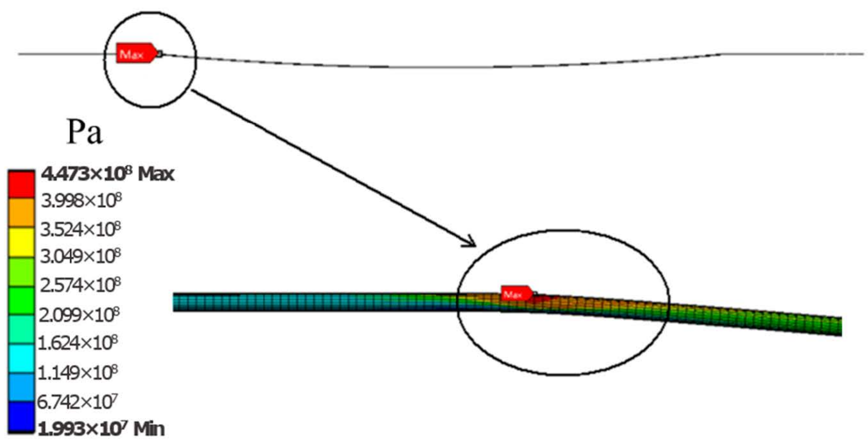

Figure 4. The ES along the pipeline.

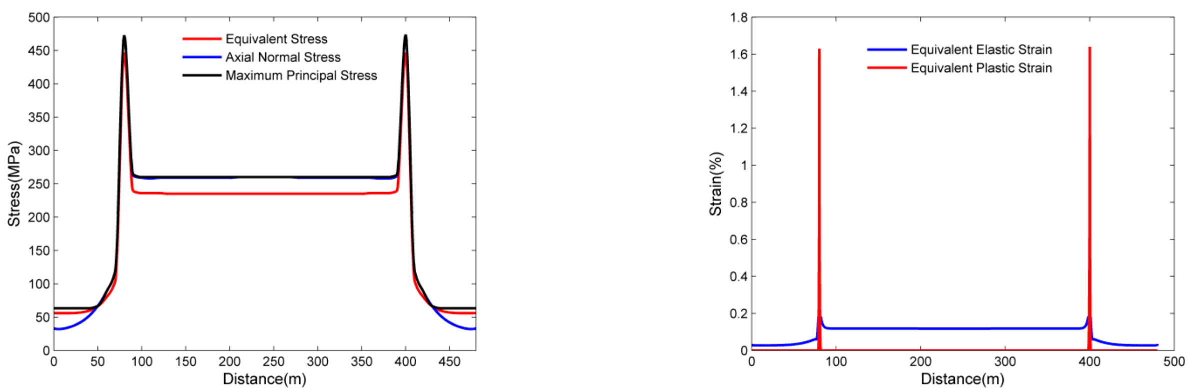

(**a**) (**b**)

Figure 5. The (**a**) stress and (**b**) strain along the pipeline.

Figure 5b depicts the elastic strain and plastic strain along the pipeline. The maximum equivalent plastic strain along the pipeline is 1.64%. The maximum equivalent elastic strain is equal to 0.22%, and they are both in critical locations. The elastic deformation is negligible compared with the plastic deformation in the critical location and other locations instead. The elastic strain remains unchanged along the suspended section other than in critical locations. The stress and strain nearly distribute symmetrically and the center is the pipe axis.

The deflection distribution along the pipeline is shown in Figure 6. The maximum deflection of this pipeline is 7.4 m, which is far more than the accepted value in oil and gas pipeline engineering. The deflection should not be more than 0.005 times the suspended length in China [40]. The deflection along the pipeline also distributes symmetrically and the maximum deflection is located at the midpoint of the suspended pipeline section. Meanwhile, the real deflection is 7.1 m, which approaches the calculation value. It concludes that the nonlinear FEM, which is employed for analyzing the suspended pipeline, has strong feasibility. As the case results by the nonlinear numerical method, the maximum equivalent stress has exceeded the yield stress of X52 and the serious plastic strain occurs in the critical location. The suspending of the pipeline can lead to serious risks to the safety operation of pipelines. Nevertheless, the failure process of the suspended pipe is unclear. In the current study, factors such as the suspended length, the ratio of diameter and thickness, and the fluid mass, which influence the failure of the suspended pipeline, are analyzed to grasp the failure mechanism and critical influence factors.

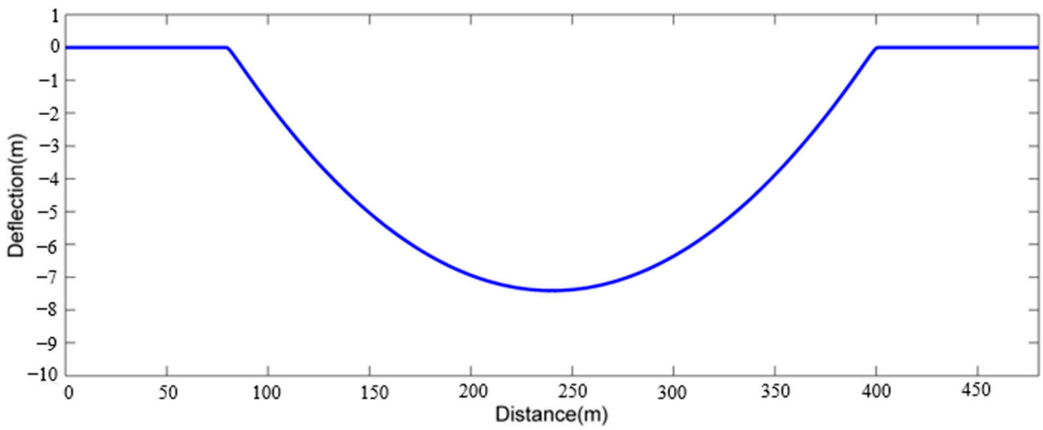

Figure 6. The distribution of the deflection along the pipeline.

3.1. The Effects of Suspended Lengths

To explore the influences of suspended lengths, results are calculated by using 219.1 mm-diameter and 6.4 mm-thickness X52 Steel pipelines with suspended lengths ranging from 50 to 320 m. The contact nonlinear and the metal plastic deformation are also considered in the numerical simulation. The soil parameters are identical to the parameters used in the last Section.

Figure 7a lists values of MES and the axial normal stress in terms of suspended length. The results show that both stresses raise with the increase in lengths. The rate of growth has a decreasing tendency and changes dramatically when the suspended length is 100 m. This result demonstrates that the pipeline suffers different deformation stages and it can also be obtained in Figure 7b.

Figure 7b depicts the values of the MES, elastic-strain, and plastic-strain in terms of the suspended length. As shown in Figure 7b, the plastic strain appears when the length exceeds 50 m. Elastic deformation is the main cause of pipeline strain when the length does not exceed 100 m, while plastic deformation becomes the dominant factor when the suspended length is over 150 m. The plastic deformation rapidly increases while the elastic changes slightly in the plastic deformation stage.

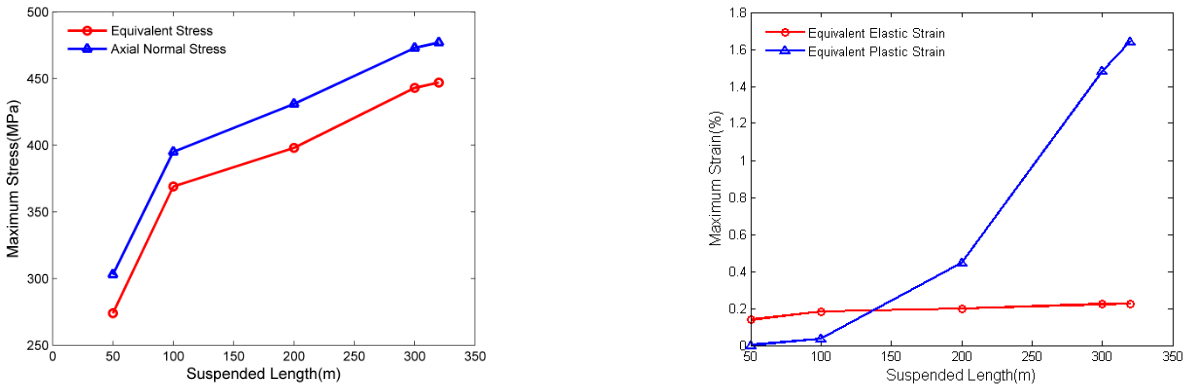

(**a**) (**b**)

Figure 7. (**a**) The MES and the ANS versus the suspended length (**b**) the maximum EES and the maximum EPS versus the suspended length.

The total strain in the critical location under different suspended lengths is illustrated in Figure 8. The critical locations rapidly enlarge with increasing the suspended length and the maximum value ranges from 0.13% to 1.87%. Figure 9 shows the deflection along the axial varies with the length. The maximum deflection of the pipeline with a 320 m suspended length improves to 7.4 m, which is 12.6 times that with a 50 m suspended length. As a result, the suspended length has a significant influence on the failure process.

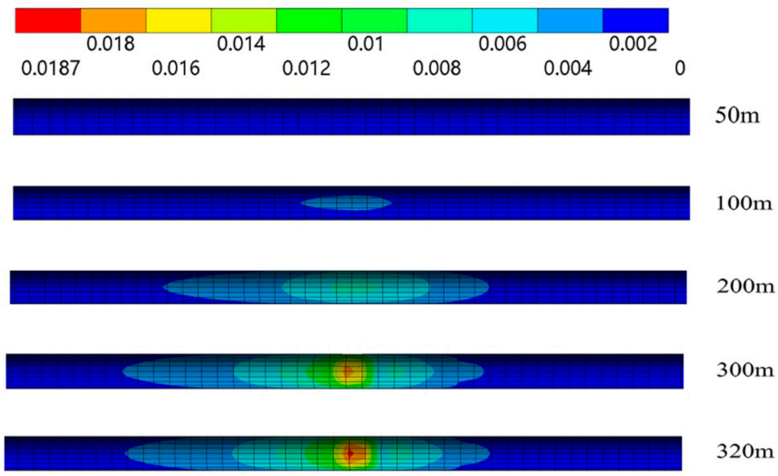

Figure 8. The total strain in the critical location versus the suspended length.

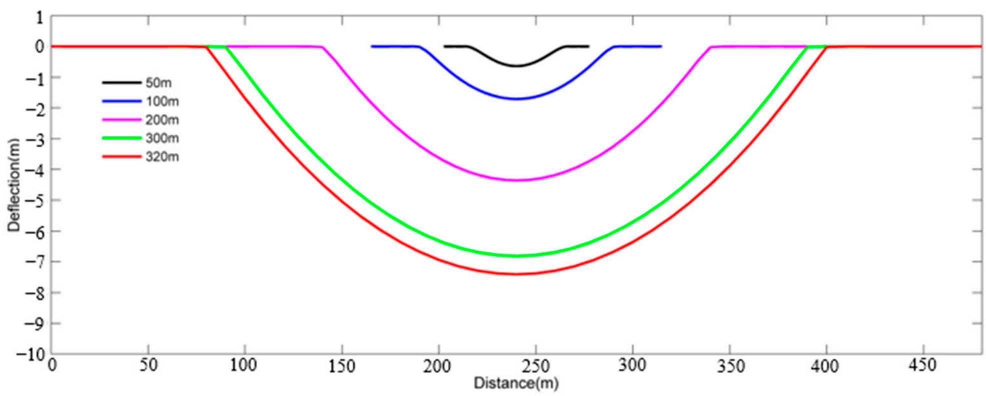

Figure 9. The deflection along axial under different values of the suspended length.

3.2. The Effects of D/t

The influence of D/t on pipeline safety status is investigated by considering different values of D/t, under an identical length, operating pressure, and soil conditions. The results are obtained for the 219.1 mm diameter X52 steel pipelines with thicknesses between 5.6 mm and 11 mm, being equivalent to D/t values from 19.9 to 39.1.

Figure 10 shows the simulation results for investigating the critical factor of D/t. Figure 10a presents the MES and the MAS versus D/t. The curves show an obvious growth with increasing values of the D/t, which implies that thin-wall and large-diameter pipelines are more likely to fracture and fail in a suspended state caused by natural disasters.

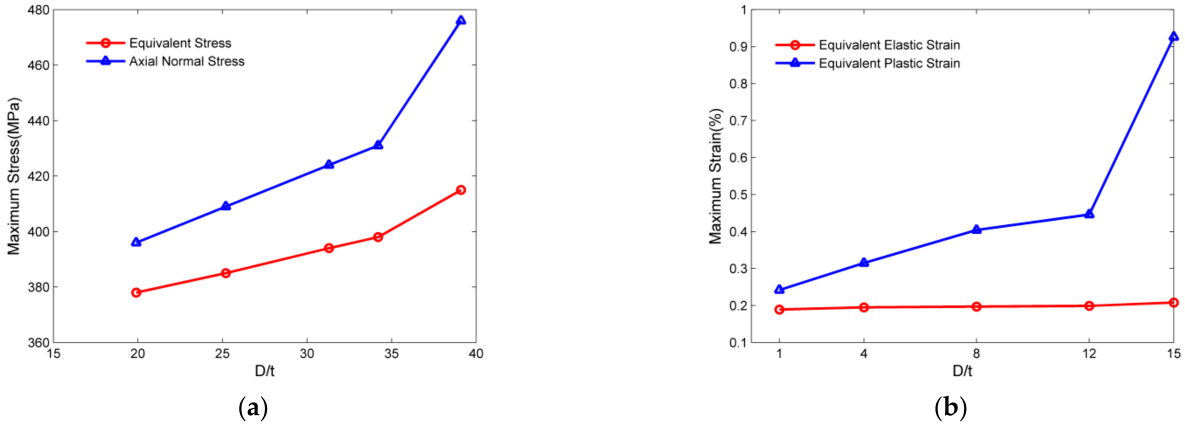

Figure 10. (**a**) The MES and the MAS versus D/t and (**b**) the elastic strain and the plastic strain versus D/t.

The Maximum Equivalent plastic strain substantially rises with the increase of D/t. The Maximum Equivalent elastic strain shows a slight increase tendency with increasing the value of D/t. The results also indicate that the critical location has gone into the plastic deformation stage, and the plastic strain is the main deformation pattern.

Figure 11 shows the influence of D/t on the total strain in the critical location. The strain quickly reaches the maximum at the end of the suspended segment and also increases with the increasing D/t. The effects of the D/t on the pipeline deflection are also shown in Figure 12. The maximum deflection raises 11.8% to 4.47 m while D/t rises from 19.9 to 39.1. The ratio effect is insignificant compared with the suspended length.

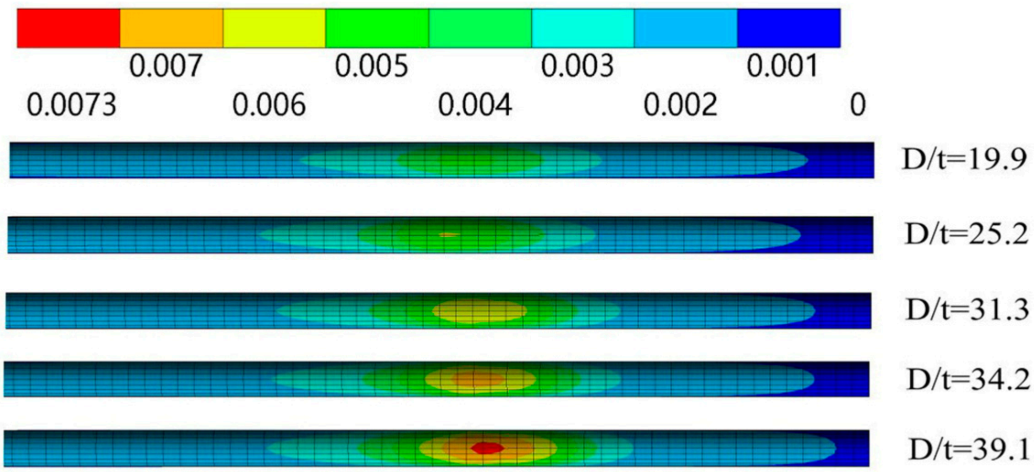

Figure 11. Total strain contours of the location of the maximum strain versus the ratio of diameter to thickness (D/t).

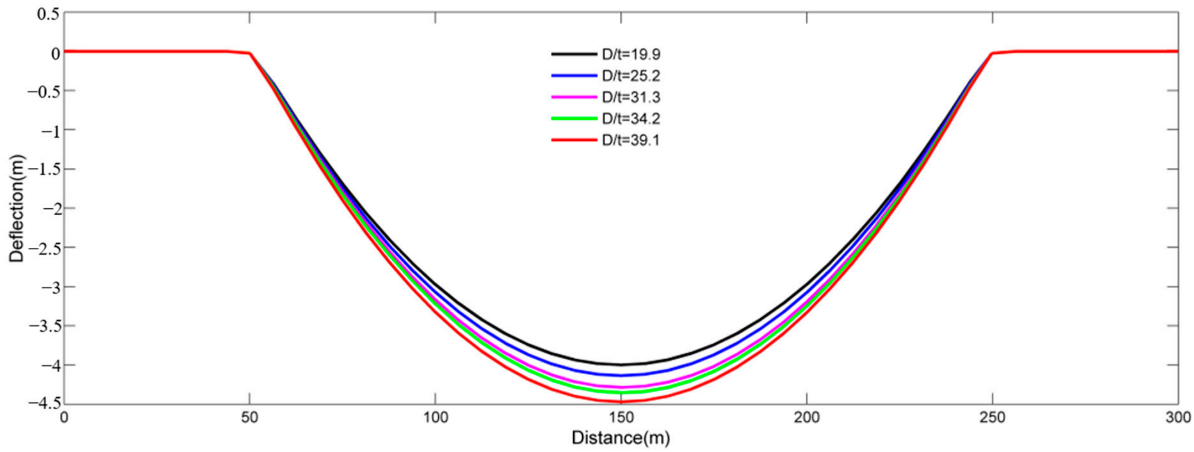

Figure 12. The deflection along axial varies with D/t.

3.3. The Effects of Operating Pressure

The influence of the operating pressure on pipe safety status is also examined by considering identical length, D/t, and other parameters. The result is obtained via 219.1 mm diameter X52 steel pipelines with a thickness of 6.4 mm. The operating pressure is the main basis of oil and gas pipeline design, and it must meet the safety requirements by the following expression [41,42]. Therefore, the maximum value of the operating pressure P_{max} is obtained as 15 MPa when the design factor is equal to the maximum (0.72).

$$P \leq F\frac{2\sigma_y t}{D} \tag{1}$$

Figure 13a presents the values of the MES and the MAS under different operating pressure. The results show that the maximum equivalent stress rises just 4.7% when the operating pressure improves sharply from 1 Mpa to 15 Mpa. As shown in Figure 13b, the equivalent plastic strain presents a low growth rate while the operating pressure is less than 12 Mpa.

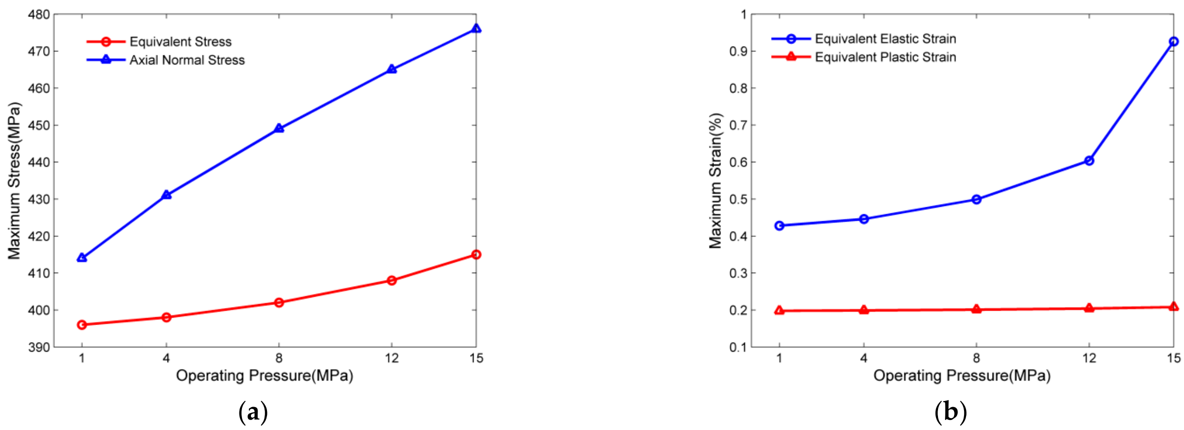

Figure 13. (**a**) The MES and the MAS versus the operating pressure and (**b**) the elastic strain and the plastic strain versus the operating pressure.

The total strain at the critical location for different operating pressure in Figure 14 also shows that the operating pressure has a slight influence on the strain. The numerical results also reveal the relation between the suspended pipeline deflection and the operating pressure in Figure 15. The maximum deflection slightly improves by 9.0% to 4.66 m while the operating pressure increases from 1 MPa to 15 MPa. Therefore, we can conclude that normal pressure is not critical for the failure of the suspended pipes.

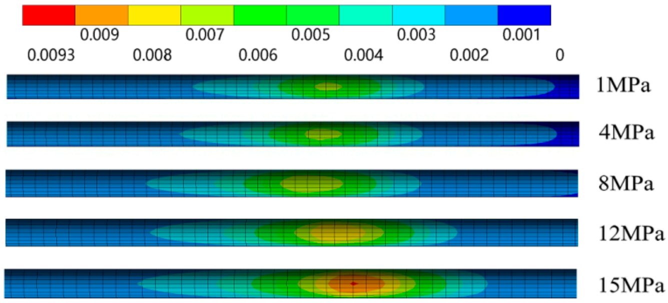

Figure 14. The total strain in the critical location versus the operating pressure.

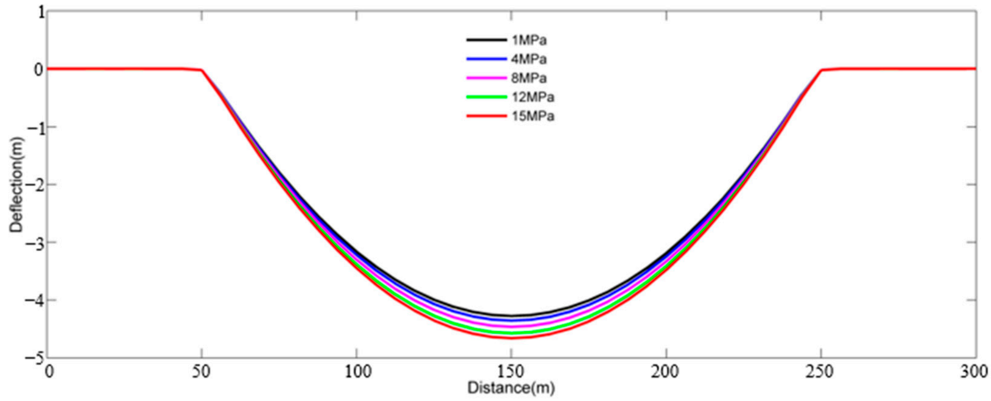

Figure 15. The deflection along axial under different values of the operating pressure.

3.4. The Effects of the Fluid Gravity

The effects of fluid gravity are investigated in this subsection. The operating pressure is the main consideration during the design of the buried pipeline without regard to the effects of the fluid gravity, as shown in Equation (1). However, the fluid gravity has an impact on the suspended pipeline resulting from the loss of the ground support, especially for the liquid pipeline as depicted in Figure 16a. The ES with fluid gravity is all greater than those without fluid gravity along the axial. The maximum relative difference is 43%, and the average relative difference value is 39% along the axial. Figure 16b shows the maximum equivalent stress in terms of the suspended length with fluid gravity and without fluid gravity. The values of the maximum equivalent stress with fluid stress are also greater than those without fluid gravity under different suspended lengths. The maximum relative difference is 40%, and the average relative difference is 19%.

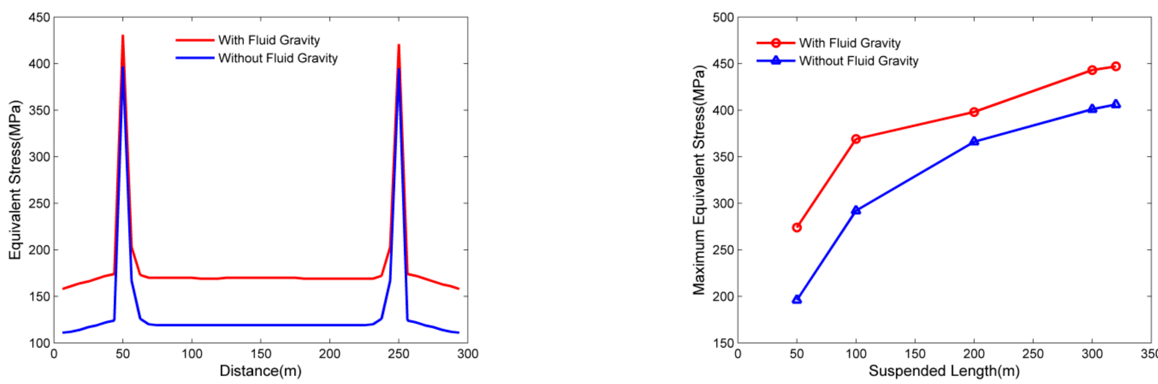

(**a**) (**b**)

Figure 16. (**a**) The equivalent stress along axial and (**b**) the maximum equivalent stress under different values of the suspended length versus the fluid gravity.

Figure 17a depicts the maximum total strain under different values of the suspended length versus fluid gravity. The results demonstrate that the strain rises with increasing length. The relative difference is 40% when the suspended length is 50 m, and the relative difference is 144%.

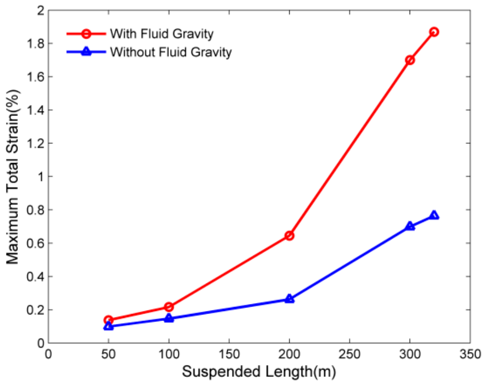

(**a**)

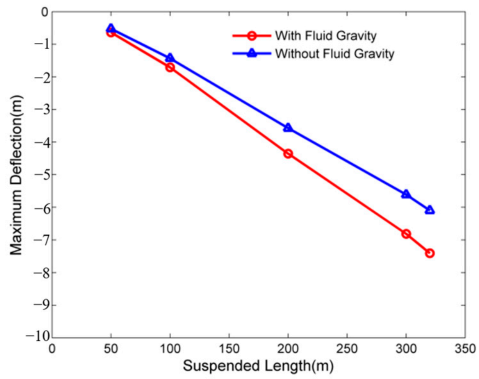

(**b**)

Figure 17. (**a**) The maximum total strain and (**b**) the maximum deflection under different values of the suspended length versus the fluid gravity.

Figure 17b shows the maximum deflection under different values of the suspended length versus fluid gravity. The total strain has a near-linear increasing tendency with increasing the suspended length. The slope with the fluid gravity is 0.025, and it is 0.021 without the fluid gravity. The absolute difference also increases with the increase in length. Therefore, The effects of fluid gravity can't be ignored especially for long-suspended pipelines.

4. Emergency Response to Suspended Pipelines Caused by Natural Disasters

4.1. Emergency Decision Criteria

According to the nonlinear FEM analysis, the pipeline's safety mainly depends upon the critical locations on the ends of the suspended section. D/t, the operating pressure, and the fluid gravity all have an impact on the plastic deformation of critical locations. The pipeline failure can be accelerated by increasing these factors. However, the suspended length plays a crucial role in pipeline failure. The pipeline appears plastic deformation when the suspended length exceeds 50 m. At present, no standard is proposed specifically for the safety evaluation and emergency response of suspended pipelines. However, for the engineer design, an analytic calculation approach for axial normal stress is provided in ASME B31.4 [41], and the axial normal stress σ_a is obtained:

$$\sigma_{\mathrm{a}} = \frac{PD}{4t} + \frac{iM}{Z} + \frac{F_a}{A} \tag{2}$$

where σ_a is the axial normal stress, MPa; A is the metal area of the nominal pipeline cross-section, mm^2; D is the diameter of the pipeline, mm; F_a is the axial force, N; and i is the component stress intensification. For a straight pipeline, i = 1.0. M is the bending moment across the nominal pipe cross-section due to weight or seismic inertia loading, N m; P is the pressure, MPa; and t is the thickness of the pipeline, mm. The bending moment M of a suspended pipeline is calculated:

$$M = \frac{ql^2}{12} \tag{3}$$

where q is the Pipeline load per unit length, including pipe gravity and fluid gravity, N/m, and l is the length, m. According to the above expressions, and regardless of the thermal stress (i = 1 and F_a = 0), the maximum allowable suspended length can be obtained.

$$l_{\max} = \sqrt{\frac{12Z\left(\sigma_y - \frac{PD}{4t}\right)}{q}} \tag{4}$$

The section modulus Z is calculated:

$$Z = \frac{\pi}{32000} D^3 \left(1 - \left(\frac{D-t}{D}\right)^4\right) \tag{5}$$

The maximum allowable suspended length of the pipeline model proposed in Section 2 is 32 m by this analytic calculation method. Compared with the result of the nonlinear FEM (50 m), the current standard for engineer design has a safety factor of 1.56 times. This stress calculation method is only appropriate for elastic deformation pipelines. The maximum permitted strain is limited to 2% if the stress is greater than the yield in ASME B31.8 [42]. Further nonlinear finite element calculation indicts that the suspended length is 340 m when the total strain is 2%. Namely, the maximum suspended length for engineer design is 50 m, and it can be 340 m for the safety limit. This result also can explain the fact that the pipeline with 320 m suspended length does not fracture. For emergency response, the pipeline is designed according to design standards, and operating pressure and D/t are conservatively designed. As a result, the emergency response for suspended pipelines caused by natural disasters should focus on the fluid inside the pipeline and the suspended length. Additionally, emergency response levels are determined based on plastic strain and suspended length.

4.2. Emergency Levels and Treatment Measures

To support the decision-making on emergency response to suspended pipelines triggered by natural disasters, emergency levels are developed according to the suspended length (Table 3). Emergency response is divided into four levels and each level has different treatment measures. Level I represents the condition in which the suspended length is no more than 50 m and there is no plastic deformation. At this level, the transportation operation can be normally conducted, and the loss of soil caused by natural disasters should be refilled as soon as possible to restore soil support to the pipeline. If the length is larger than 50 m, the plastic strain may occur while it is not dominant until the suspended length is larger than 150 m. This emergency condition is called Level II, in which the transportation operations should be interrupted to reduce the risk and the loosed soil should be filled to restore the stress status of the pipeline as soon as possible. Level III indicates the strain is dominated by plastic deformation, while the strain is less than 2% when the suspended length is larger than 150 m and less than 340 m. In Level III, the pipeline should be replaced before the restoration of soil support. If the suspended length is larger than 340 m and the strain exceeds 2%, the rupture risk is very high, and additional measures should be taken to deal with possible major accidents such as a leak, fire, and explosion.

Table 3. Emergency response levels and treatment measures.

Emergency Levels	Descriptions	Treatment Measures
I $l < 50$ m	Low risk, no plastic strain.	Normal transportation operations, refill the soil in the suspended section.
II 50 m$\leq$ l < 150 m	Medium risk, there are elastic strain and plastic strain, while mainly elastic deformation.	Stop transportation operations and refill the soil in the suspended section as soon as possible.
III 150 m$\leq l <$ 340 m	High-risk, plastic strain is dominant but the strain is less than 2%.	Stop transportation operations, replace the suspended pipe, and refill the soil in the suspended section.
IV $l \geq 340$ m	Very high risk, with a strain larger than 2%, and even causes oil leakage, fire, and explosion.	Stop transportation operations, evacuate surrounding people, prepare for leakage rescue, fill the soil in the suspended section, and replace the suspended pipe.

5. Conclusions

To deal with the frequent accidents of suspended pipelines triggered by natural disasters, a safety analysis of suspended pipelines on the basis of a nonlinear FEM is conducted and an emergency response plan is proposed based on the safety analysis. The nonlinear FEM is proposed to analyze the failure mechanisms of suspended pipelines and support decision making during emergency response.

(1) The finite element results show that the case pipeline with 320 m suspended length is in a high-risk status with a 447 MPa equivalent stress and 1.8% total strain at the critical locations.
(2) The stress, strain, and deflection are symmetrical along the perpendicular bisector of the pipeline. Both the maximum stress and strain appear at the ends of the suspended section, which are defined as critical locations, and the safety of suspended pipelines depends on the locations.
(3) The factors of suspended length, the ratio of diameter to thickness, the internal pressure, and the fluid inside the pipe influence the safety of suspended pipelines. The pipeline stress, strain, and deflection increase with increasing these factors. The suspended length is the most critical factor for the safety of the suspended pipeline.
(4) The irreversible plastic strain occur if the suspended length exceeds 50 m and becomes dominant when the length exceeds 150 m, and the total strain reaches 2% when the suspended length is 340 m.
(5) An emergency plan with four emergency levels based on plastic strain and suspended length is developed to deal with different suspended pipelines caused by natural disasters.
(6) This study only considers the X52 steel, and thus, other steels such as x70 and x80 may be considered in the future. Additionally, the coupling effects of different natural disasters and hazardous scenarios may also be considered to improve the application of this study. In addition, this study may be extended to analyze submarine pipelines by changing the model parameters such as loads and boundary conditions.

Author Contributions: Methodology, C.L.; Writing – original draft, J.Y.; Writing – review & editing, C.C. All authors have read and agreed to the published version of the manuscript.

Funding: This research was funded by the Science and Technology Department of Sichuan Province, grant number (23ZDYF1671).

Conflicts of Interest: The authors declare no conflict of interest.

References

1. Dale, S. *BP Statistical Review of World Energy 2022*; World Petroleum Congress: London, UK, 2022.
2. Li, X.; Zhang, Y.; Abbassi, R.; Khan, F.; Chen, G. Probabilistic fatigue failure assessment of free spanning subsea pipeline using dynamic Bayesian network. *Ocean. Eng.* **2021**, *234*, 109323. [CrossRef]
3. Chen, C.; Li, C.; Reniers, G.; Yang, F. Safety and security of oil and gas pipeline transportation: A systematic analysis of research trends and future needs using WoS. *J. Clean. Prod.* **2021**, *279*, 123583. [CrossRef]
4. Zhang, M.; Ling, J.; Tang, B.; Dong, S.; Zhang, L. A Data-Driven Based Method for Pipeline Additional Stress Prediction Subject to Landslide Geohazards. *Sustainability* **2022**, *14*, 11999. [CrossRef]
5. Wang, Y.; Li, R.; Xia, A.; Ni, P.; Qin, G. An integrated modeling method of uncertainties: Application-orientated fuzzy random spatiotemporal analysis of pipeline structures. *Tunn. Undergr. Space Technol.* **2023**, *131*, 104825. [CrossRef]
6. Wang, Y.; Xia, A.; Qin, G. Probabilistic modeling for reliability analysis of buried pipelines subjected to spatiotemporal earthquakes. *Probabilistic Eng. Mech.* **2022**, *69*, 103315. [CrossRef]
7. The Xinhua News Agency. Serious Risk in Shiting River Section of Lanzhou-Chengdu-Chongqing Refined Oil Pipeline Caused by Rainstorm in Sichuan. 2013. Available online: http://www.gov.cn/jrzg/2013-07/13/content_2447010.htm (accessed on 6 December 2022).
8. Qilu Evening News. The Gas Pipeline Near a Gas Station Leaked Suddenly Due to Ground Subsidence. Available online: https://www.chinanews.com/sh/2014/03-06/5918827.shtml (accessed on 5 December 2022).
9. Shittu, A.A.; Kara, F.; Aliyu, A.; Unaeze, O. Review of pipeline span analysis. *World J. Eng.* **2019**, *16*, 166–190. [CrossRef]
10. Wu, X.N.; Lu, H.F.; Wu, S.J.; Kun, H.; Chen, X.; Kang, F.X.; Liu, Z.L. Analysis of Suspended Pipeline Stress Sensitivity. *Appl. Mech. Mater.* **2014**, *501–504*, 2331–2334. [CrossRef]

11. Zhang, L.; Xie, Y.; Yan, X.; Yang, X. An elastoplastic semi-analytical method to analyze the plastic mechanical behavior of buried pipelines under landslides considering operating loads. *J. Nat. Gas Sci. Eng.* **2016**, *28*, 121–131. [CrossRef]
12. Peng, S.; Luo, Y. Determination of stress field in buried thin pipelines resulting from ground subsidence due to longwall mining. *Min. Sci. Technol.* **1988**, *6*, 205–216. [CrossRef]
13. Cao, Z.; Zhou, Y.; Xu, P.; Li, J. Mechanical Response Analysis and Safety Assessment of Shallow-Buried Pipeline under the Influence of Mining. *CMES Comput. Model. Eng. Sci.* **2014**, *101*, 351–364.
14. Karamitros, D.; Bouckovalas, G.; Kouretzis, G.; Gkesouli, V. An analytical method for strength verification of buried steel pipelines at normal fault crossings. *Soil Dyn. Earthq. Eng.* **2011**, *31*, 1452–1464. [CrossRef]
15. Hendriks, M.A.; 't Hart, C.M.P.; Frissen, C.M. Elasto-plastic design and assessment of pipelines: 3D finite element modeling. In Proceedings of the ASCE Pipeline Division Specialty Congress-Pipeline Engineering and Construction, San Diego, CA, USA, 1–4 August 2004; pp. 923–932.
16. Trifonov, O.V.; Cherniy, V.P. Elastoplastic stress–strain analysis of buried steel pipelines subjected to fault displacements with account for service loads. *Soil Dyn. Earthq. Eng.* **2012**, *33*, 54–62. [CrossRef]
17. Trifonov, O.V.; Cherniy, V.P. A semi-analytical approach to a nonlinear stress–strain analysis of buried steel pipelines crossing active faults. *Soil Dyn. Earthq. Eng.* **2010**, *30*, 1298–1308. [CrossRef]
18. Zhang, Z.; Lv, X.; Mao, M.; Pan, Y.; Fang, L.; Wu, Z. Mechanical response for rainfall-induced landslides on jointed gas pipelines. *Comput. Geotech.* **2022**, *146*, 104708. [CrossRef]
19. Liao, K.; Li, Y.; Yao, Q. Calculation and Analysis for Critical Parameters of Long-Span Suspended Pipeline Stress Deformation Area. In Proceedings of the International Conference on Pipelines and Trenchless Technology 2011, Beijing, China, 26–29 October 2011; American Society of Civil Engineers: Reston, VA, USA, 2011.
20. Zhao, K.; Xiong, H.; Chen, G.; Zhao, D.; Chen, W.; Du, X. Wave-induced dynamics of marine pipelines in liquefiable seabed. *Coast. Eng.* **2018**, *140*, 100–113. [CrossRef]
21. Wang, Q.; Bian, J.; Huang, W.; Lu, Q.; Zhao, K.; Li, Z. Seabed Liquefaction around Pipeline with Backfilling Trench Subjected to Strong Earthquake Motions. *Sustainability* **2022**, *14*, 12825. [CrossRef]
22. Huang, Y.; Qin, G.; Hu, G. Failure pressure prediction by defect assessment and finite element modelling on pipelines containing a dent-corrosion defect. *Ocean Eng.* **2022**, *266*, 112875. [CrossRef]
23. Wang, X.; Shuai, J.; Ye, Y.; Zuo, S. Investigating the Effects of Mining Subsidence on Buried Pipeline Using Finite Element Modeling. In Proceedings of the 2008 7th International Pipeline Conference: American Society of Mechanical Engineers, Calgary, AB, Canada, 29 September–3 October 2008; pp. 601–606.
24. Zakeri, A. Submarine debris flow impact on suspended (free-span) pipelines: Normal and longitudinal drag forces. *Ocean Eng.* **2009**, *36*, 489–499. [CrossRef]
25. Shao, B.; Yan, X.Z.; Yang, X.J. Nonlinear Dynamic Response and Safety Analysis of Suspended Submarine Pipeline. *Appl. Mech. Mater.* **2011**, *121–126*, 3366–3370. [CrossRef]
26. Kunert, H.; Otegui, J.; Marquez, A. Nonlinear FEM strategies for modeling pipe–soil interaction. *Eng. Fail. Anal.* **2012**, *24*, 46–56. [CrossRef]
27. Zhang, Y.; Yi, D.; Xiao, Z.; Huang, Z. Engineering critical assessment for offshore pipelines with 3-D elliptical embedded cracks. *Eng. Fail. Anal.* **2015**, *51*, 37–54. [CrossRef]
28. Saeedzadeh, R.; Hataf, N. Uplift response of buried pipelines in saturated sand deposit under earthquake loading. *Soil Dyn. Earthq. Eng.* **2011**, *31*, 1378–1384. [CrossRef]
29. Zheng, J.; Zhang, B.; Liu, P.; Wu, L. Failure analysis and safety evaluation of buried pipeline due to deflection of landslide process. *Eng. Fail. Anal.* **2012**, *25*, 156–168. [CrossRef]
30. Zhang, J.; Liang, Z.; Han, C. Buckling behavior analysis of buried gas pipeline under strike-slip fault displacement. *J. Nat. Gas Sci. Eng.* **2014**, *21*, 921–928. [CrossRef]
31. Liu, X.; Ai, Z.; Qi, J.; Wang, S.; Qin, H.; Qian, H. Mechanics analysis of pipe lifting in horizontal directional drilling. *J. Nat. Gas Sci. Eng.* **2016**, *31*, 272–282. [CrossRef]
32. Vazouras, P.; Dakoulas, P.; Karamanos, S.A. Pipe–soil interaction and pipeline performance under strike–slip fault movements. *Soil Dyn. Earthq. Eng.* **2015**, *72*, 48–65. [CrossRef]
33. Mehrjardi, G.T.; Karimi, M. Numerical Modeling of Buried Steel Pipe Subjected to Impact Load. *J. Pipeline Syst. Eng. Pract.* **2021**, *12*, 04021048. [CrossRef]
34. Ma, H.; He, B.; Luo, X.; Cai, W.; Liu, D.; Hou, C.; Han, J. Investigation on strain characteristic of buried natural gas pipeline under longitudinal landslide debris flow. *J. Nat. Gas Sci. Eng.* **2021**, *86*, 103708. [CrossRef]
35. Cheng, P.; Guo, J.; Yao, K.; Liu, C.; Liu, X.; Liu, F. Uplift Behavior of Pipelines Buried at Various Depths in Spatially Varying Clayey Seabed. *Sustainability* **2022**, *14*, 8139. [CrossRef]
36. Tsatsis, A.; Alvertos, A.; Gerolymos, N. Fragility analysis of a pipeline under slope failure-induced displacements occurring parallel to its axis. *Eng. Struct.* **2022**, *262*, 114331. [CrossRef]
37. Wu, Y.; Meng, B.; Wang, L.; Qin, G. Seismic vulnerability analysis of buried polyethylene pipeline based on finite element method. *Int. J. Press. Vessel. Pip.* **2020**, *187*, 104167. [CrossRef]
38. Zheng, T.; Liang, Z.; Zhang, L.; Tang, S.; Cui, Z. Safety assessment of buried natural gas pipelines with corrosion defects under the ground settlement. *Eng. Fail. Anal.* **2021**, *129*, 105663. [CrossRef]

39. Lawrence, K.L. *ANSYS Workbench Tutorial Release 14*; SDC Publications: Mission, KS, USA, 2012.
40. Shi, Z. *Power Pipeline Design Manual*; China Machine Press: Beijing, China, 2006.
41. Institute ANS. *Pipeline Transportation Systems for Liquid Hydrocarbons and Other Liquids*; American Society of Mechanical Engineers: New York, NY, USA, 2012.
42. Institute ANS. *Gas Transmission and Distribution Piping Systems*; American Society of Mechanical Engineers: New York, NY, USA, 2012.